Materials Today Bio 25 (2024) 100961

Contents lists available at ScienceDirect

Materials Today Bio

journal homepage: www.journals.elsevier.com/materials-today-bio

Biostable hydrogels consisting of hybrid β-sheet fibrils assembled by a pair of enantiomeric peptides

Tingyuan Tan [a], Yangqian Hou [b], Jiali Shi [b], Biao Wang [a,*], Yi Zhang [b,**]

[a] Research Institute of Interdisciplinary Sciences & School of Materials Science and Engineering, Dongguan University of Technology, Dongguan, 523808, China
[b] Shanghai Institute of Applied Physics, Chinese Academy of Sciences, Shanghai, 201800, China

ARTICLE INFO

Keywords:
Molecular chirality
Hydrogel
Peptide
Co-assembly

ABSTRACT

The assembly of chiral peptides facilitates the formation of diverse supramolecular structures with unique physicochemical and biological properties. However, the effects of chirality on peptide assembly and resulting hydrogel properties remain underexplored. In this study, we systematically investigated the assembly propensity, morphology, and biostability of mixture of a pair of enantiomeric peptides $^{L}E^{L}C^{L}A^{L}F^{L}F$ (ECF-5) and $^{D}E^{D}C^{D}A^{D}F^{D}F$ (ecf-5) at various ratios. Results indicate the development of β-sheet fibrils, ultimately leading to the formation of self-supporting hybrid hydrogels. The hydrogel formed at a ratio of 1:1 exhibits a significantly lower storage modulus (G′) than of the ratios of 0:1, 1:3, 3:1 and 1:0 (n_D/n_L; same below). Kink-separated fragments of approximately 100 nm in length predominate at ratios of 1:3 and 3:1, compared with the smooth fibrils at other ratios, probably attributed to an alternating arrangement of the co-assembled and self-assembled peptide fragments. The introduction of ecf-5 to the hybrid hydrogels improves resistance to proteolytic digestion and maintains commendable biocompatibility in both MIN6 and HUVECs cells. These findings provide valuable insights into the development of hydrogels with tailored properties, positing them potential scaffolds for 3D cell culture and tissue engineering.

1. Introduction

Chirality is a ubiquitous selection in the organization of natural and artificial systems [1–3]. Specifically, proteins are predominantly encoded by L-amino acids [4,5], resulting in distinctive features recognized by biological systems and susceptible to degradation by intracellular enzymes [6]. The atomically resolved structures of functional proteins further reveal the widespread prevalence of chirality in almost all signal transduction systems [7]. The inherent chirality of the peptides and proteins not only offers insights into fundamental biological processes but also presents opportunities for advancing supramolecular biomaterials. These materials are characterized by different fibril handedness [8], proteolytic susceptibility [9], and bioactivity [10], providing a versatile platform for various applications in chiral recognition [11,12], catalysis [13], cancer therapeutics [14], antimicrobial activity [15–17], and 3D cell culture [18,19].

Supramolecular hydrogels derived from peptides and proteins have garnered considerable attention due to their capacity to mimic the essential properties of native extracellular matrix (ECM) [20,21]. This ability to mimic is particularly significant in nanobiotechnology and biological engineering [22–28], owing to the favorable biocompatibility, ease of chemical modification, diversity of amino acids and ease of fabrication associated with these hydrogels [29]. It is crucial to control the mechanical properties (high stiffness, shear thinning, and rapid recovery) of peptide/protein hydrogels, which are intricately governed by the stiffness of the self-assembled fibrils and their cross-linking networks [30,31]. To improve hydrogels' performance, one needs to involve the aromatic amino acid residues or synthetic terminal groups into short peptides, allowing for the introduction of π-π stacking and hydrophobic interactions to enhance their assembly capacities [32,33]. However, the effect of these synthetic terminal groups should be carefully considered when applied in biological fields, particularly *in vivo* [34–37]. Furthermore, minor alterations in peptide sequences could significantly influence the assembly process [38], making it challenging to predict gel formation and develop hydrogels with desired properties [34]. Most importantly, the rapid degradation of L-peptide hydrogels poses an obstacle to their applications in tissue engineering and regenerative medicine [39].

* Corresponding author.
** Corresponding author.
E-mail addresses: wangbiao@mail.sysu.edu.cn (B. Wang), zhangyi@sinap.ac.cn (Y. Zhang).

https://doi.org/10.1016/j.mtbio.2024.100961
Received 16 October 2023; Received in revised form 22 December 2023; Accepted 15 January 2024
Available online 17 January 2024

The involvement of peptides, composed of unnatural D-amino acids, represents an established approach to developing advanced supramolecular hydrogels and regulating the degradation of their scaffolds, yielding accelerated gelation, heightened therapeutic potential, and improved stability, which are beneficial for applications in drug delivery *in vivo* and cell culture *in vitro* [37,40]. A combination of D- and L-amino acids in heterochiral sequences is effective in constructing resilient supramolecular architectures, despite the individual enantiomers being unable to self-assemble [41]. The amphiphilic peptide KFE8 (Ac-FK-FEFKFE-NH_2), consisting of two FKFE repeat motifs with opposite chirality was capable of assembling into helical taps with dimensions surpassing those of their fibrillar homochiral counterpats [42]. The derivative DP06, whose L-lysine and L-arginine residues were substituted with D-amino acids, displayed remarkable stability and minimal toxicity *in vitro* [43]. The co-assembly of homochiral enantiomers of peptides has emerged as a versatile strategy for generating supramolecular structures with unique characteristics, distinct from enantiomeric aggregation, such as mechanical rigidity, high aggregation propensity and proteolytic susceptibility [44]. For example, an equimolar mixture of the enantiomeric amphiphilic peptides (Ac-$(FKFE)_2$-NH_2) gave rise to a new type of fibril composed of alternating L- and D-peptides in a "rippled β-sheet" orientation [30]. The rigid hydrogels were made from enantiomeric mixture of self-assembling β-hairpins [45]. Progress motivated us to incorporate D-amino acids into short peptides to explore the role of chirality in controlling emergent properties of peptide biomaterials, such as the effect of mixing ratios on the structures and performance of hydrogels co-assembled by a pair of enantiomeric peptides.

Previous research reported a biodegradable supramolecular hydrogel based on the peptide ECF-5 ($^{L}E^{L}C^{L}A^{L}F^{L}F$) as a culture scaffold for cardiomycytes [46]. Unfortunately, the limited biostability of this peptide hindered its potential to support cell growth, resulting in cell spheroids with a diameter of only 150 μm. In this study, we investigated the molecular packing, assembly propensity, morphology and biostability of the assemblies formed by mixture of ECF-5 and its enantiomer $^{D}E^{D}C^{D}A^{D}F^{D}F$ (termed as ecf-5) at various ratios. We found the formation of β-sheet fibril networks in all hydrogels. The ecf-5 and ECF-5 preferentially co-assembled into smooth fibrils at a mixing ratio of 1:1, ultimately leading to the formation of hydrogels with a lower mechanical strength. In contrast, distinctive kinks were observed on fibrils formed at unequal ratios (1:3 and 3:1), possibly attributed to the alternating arrangement of the co-assembled and self-assembled peptide fragments. All hydrogels demonstrated minimal cytotoxicity, and those with a higher proportion of ecf-5 peptide exhibited enhanced resistance to proteolytic degradation. The successful co-assembly of the enantiomeric peptides may foster the design of hydrogels with desired properties, making them promising scaffolds for 3D cell culture and tissue engineering.

2. Experimental section

2.1. Materials

The peptides ECF-5 ($^{L}E^{L}C^{L}A^{L}F^{L}F$) and ecf-5 ($^{D}E^{D}C^{D}A^{D}F^{D}F$), with a purity of 97 % confirmed by Reverse Phase High Performance Liquid Chromatography (RP-HPLC) and Electro Spray Ionization-Mass Spectroscopy (ESI-MS), were synthesized using the standard Fmoc solid phase synthesis method, as described previously [47]. These chiral peptides were stored at −20 °C. Phosphate Buffer Saline (PBS) was purchased from Sinopharm Chemical Reagent (China). Dimethyl sulfoxide (DMSO) was acquired from Sigma Aldrich Corporation (USA). The Cell Counting Kit-8 (CCK-8) was purchased from Beyotime Biotechnology (China).

2.2. Peptide assembly

ECF-5 and ecf-5 powders were dissolved in DMSO and subjected to a short vortex treatment to prepare a stock solution with a concentration of 200 mg ml^{-1}, respectively. The aforementioned solutions were mixed at various molar ratios (ecf-5: ECF-5 = 0:1, 1:3, 1:1, 3:1, and 1:0, n/n) to yield chiral peptide mixture. A certain volume of the resulting mixture was introduced to PBS to prepare assembled samples, and then stored for 24 h at room temperature. The formation of hydrogels was determined by the vial-inverted method. All hydrogel samples were prepared with a final concentration of 10 mg ml^{-1}, unless otherwise specified.

2.3. Rheology measurements

The mechanical properties of hydrogels formed by ECF-5 and ecf-5 were determined through dynamic rheological studies using a rotational rheometer (MCR 302, Anton Paar, Austria) equipped with a sample plate in parallel geometry. The hydrogel sample (10 mg ml^{-1}) was loaded onto the sample plate at 25 °C. A strain sweep experiment was conducted to identify the linear viscoelastic (LVE) regime of the hydrogel at a constant frequency of 1 Hz. Then, a frequency sweep was performed from 0.1 to 100 Hz to determine the storage modulus (G′) and loss modulus (G″) at a constant strain of 0.2 %.

2.4. Scanning electron microscopy (SEM)

The morphologies of the peptide hydrogels were observed using a Carl Zeiss AG, LEO 1530VP SEM. In brief, a certain quantity of hydrogels was deposited onto silicon wafers and allowed to absorb for 5 min. The samples were then pre-frozen at −80 °C for 1 h and subjected to a freeze-drying treatment for 24 h. Before observation, a thin layer of gold was sputter-coated onto the surface of the dried samples.

2.5. Transmission electron microscopy (TEM)

TEM experiments were conducted on a Tecnai G2 Spirit TEM (FEI, USA) with an accelerating voltage of 120 kV. The hydrogels, prepared as described above, were dispersed in Milli-Q water to obtain an aqueous solution with a peptide concentration of 2 mg ml^{-1}. A 10 μl peptide dispersion (2 mg ml^{-1}) was then dropped onto the carbon-coated 400-mesh copper grids and allowed to absorb for 30 min to ensure that the grids were fully filled with peptide samples. Subsequently, the samples were negatively stained with a 10 μl aqueous solution of uranyl acetate (1 %, w/v) for approximately 1.5 min, washed twice with water, and excess liquid was removed with filter papers. The naturally dried samples were observed by TEM under vacuum.

2.6. Atomic force microscopy (AFM)

The morphologies of the peptide assemblies were characterized by a commercial AFM instrument (Nanoscope VIII, Bruker) equipped with a 100-μm scanner. PeakForce Quantitative Nanomechanical Mapping (PF-QNM) mode was employed to visualize the morphology of peptide assemblies. Silicon cantilevers (XSC11, MikroMasch) with a nominal spring constant of 48 N m^{-1} were used. The samples were prepared by dropping 10 μl of the peptide solution (2 mg ml^{-1}) on a freshly cleaved mica substrate, followed by absorption and air-drying. The Nanoscope Software (Nanoscope Analysis Version 1.40) was utilized to analyze all images, which were not processed in any other way than flatting processing.

2.7. Thioflavin T (ThT) fluorescence measurement

ThT fluorescence measurements were carried out to monitor the β-sheet formation in the peptide hydrogels/solutions. ThT is a benzotheiazole fluorescent probe, whose fluorescence signal is sensitive to the formation of β-sheet structure in peptides [48]. The aggregation kinetics of ECF-5 and ecf-5 were monitored by introducing ThT dye. The fluorescence intensity versus time was recorded at room temperature using a

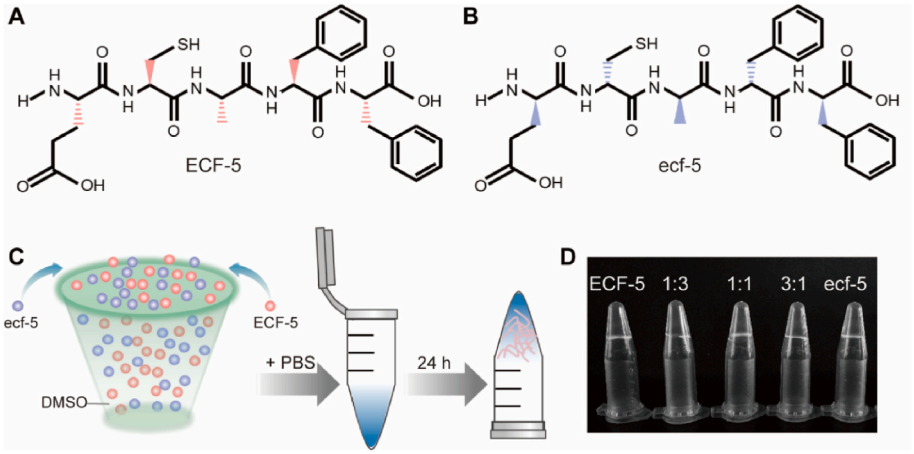

Fig. 1. Hydrogel formation of chiral peptides. (A, B) Chemical structures of ECF-5 (A) and ecf-5 (B). (C) Schematic drawing indicating the gel preparation procedure. (D) Optical images of hydrogels in the inverted vials. The number ratios shown in (D) are the molar ratios of ecf-5: ECF-5 in the peptide hydrogels; The same below unless specifically stated.

Thermo Scientific Fluoroskan Ascent (Thermo Fisher Scientific, USA) in quiescence, with an excitation at 440 nm and an emission at 485 nm. Fluorescence intensity was measured immediately following the addition of ThT to prevent fluorescence quenching. ThT fluorescence spectroscopy probed the of hydrogel dispersions composed of various ratios of ecf-5 and ECF-5. The sample was prepared by diluting the hydrogel with PBS to a dispersion with a concentration of about 2 mg ml^{-1}, and ThT dye was introduced into the dispersed solution at a final concentration of 75 μM. Fluorescence spectra were monitored with an excitation at 440 nm.

2.8. Fourier transform infra-red (FTIR) spectroscopy

FTIR spectroscopy measurements of the peptide samples were conducted using a Nicolet iZ10 Fourier transform infrared spectrometer (Thermo Fisher Scientific, USA). The preformed hydrogels (10 mg ml^{-1}), co-assembled by ecf-5 and ECF-5 at various ratios, were freeze-dried into powders. Then, Attenuated Total Reflectance (ATR)-FTIR spectroscopy of the sample was monitored in the wavenumbers ranging from 1700 to 1600 cm^{-1}. The secondary structures of chiral peptides were analyzed using Origin software.

2.9. Biostability test

Protease K (3.2 U/ml) was introduced to the hydrogels formed by combining ecf-5 and ECF-5 peptides at various ratios and incubated at 37 °C. At intervals of 0, 5, 12, and 24 h, the decompositions of the hydrogels were monitored and photographed.

2.10. Cellular toxicity

For *in vitro* cytotoxicity studies, mouse insulinoma cells (MIN6) were cultured in RPMI-1640 medium supplemented with 10 % fetal bovine serum and 50 μM β-mercaptoethanol, which was procured from Fu Heng Biology (Shanghai, China). The cell lines were passaged every 2–3 days, and the passage number did not exceed 20. For the viability assay, a transparent 96-well plate (Costar) was seeded with 2×10^4 cells in each well, and further incubated for 12 h in a 37 °C incubator containing 5 % CO_2. Then, a certain amount of freshly prepared solutions of ecf-5 and ECF-5 at different ratios was added to each well. After 24 h of cell culture, 10 μl of the enhanced Cell Counting Kit-8 (CCK-8, Beyotime, China) was added into each well, and the optical density at 450 nm (OD_{450nm}) was quantified using the Operetta CLS High-Content analyzer (PerkinElmer) at 37 °C. All samples were assayed in triplicate, and untreated cells containing the medium were used as controls. In addition, Human Umbilical Vein Endothelial Cells (HUVECs) were purchased from IMMOCELL (Guangzhou, China) and cultured in DMEM medium with 10 % fetal bovine serum and 4.5 g/L glucose. The viability assay of HUVECs treated with the chiral peptides was conducted using the same procedures as those of MIN6 cells.

3. Results and discussion

3.1. Gelation behaviors of ecf-5 and ECF-5

The chemical structures of a pair of enantiomeric peptides, namely ecf-5 and ECF-5, are depicted in Fig. 1A and B, respectively. Both peptides contain a Phe-Phe motif, which promotes their self-assembly into hydrogels. Additionally, the presence of a reductive –SH group on the Cys residue is advantageous in mitigating cellular damage induced by

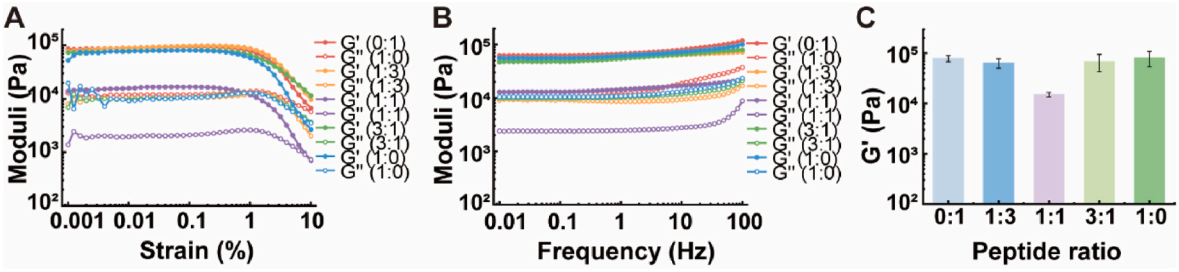

Fig. 2. Rheological measurements of hydrogels formed by chiral peptides at various molar ratios. (A) Strain sweep at a constant frequency of 1 Hz. (B) Frequency sweep at a strain of 0.2 %. (C) G′ values obtained from frequency sweep study.

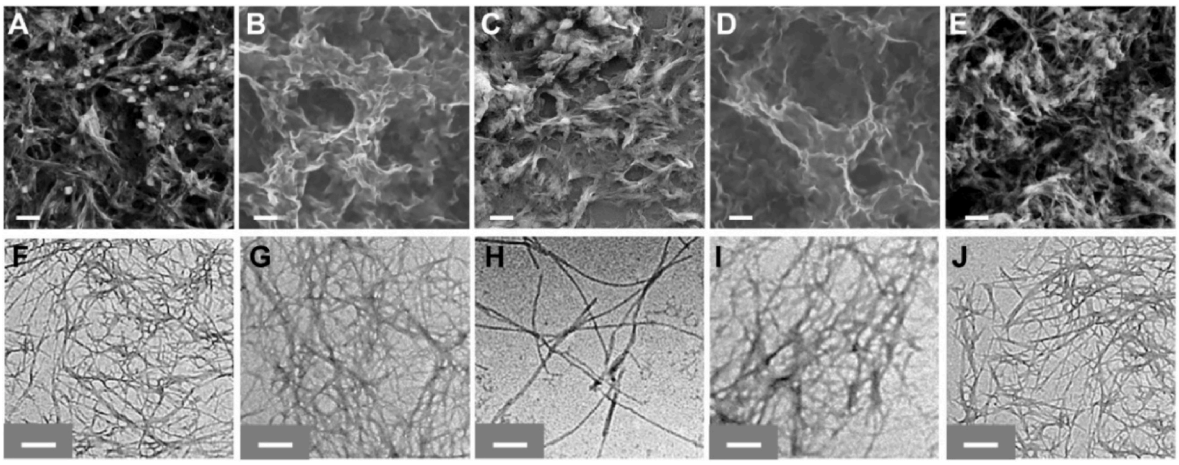

Fig. 3. SEM (A–E) and TEM (F–J) images of peptide assemblies formed by ecf-5 and ECF-5 at various ratios. (A) and (F) 0:1; (B) and (G) 1:3; (C) and (H) 1:1; (D) and (I) 3:1; (E) and (J) 1:0. The length scale bars represent 1 μm in SEM images (A–E) and 200 nm in TEM images (F–J).

oxidative stress [46]. The generation of peptide hydrogels was accomplished through a solvent switching method and evaluated by a vial-inverted method. Briefly, to prepare hydrogels, DMSO solutions (200 mg ml^{-1}) of ecf-5 and ECF-5 were mixed at various molar ratios and subsequently diluted with PBS to a peptide concentration of 10 mg ml^{-1}. The resulting mixture was allowed to be placed at room temperature for 24 h for the formation of peptide hydrogels (Fig. 1C). A vial-inverted experiment showed that mixture of ecf-5 and ECF-5 produced self-supporting hydrogels (Fig. 1D). These hydrogels remained quite stable for several months at room temperature.

To evaluate the mechanical properties of these hydrogels, rheological measurements were performed using a rotational rheometer at 25 °C. Oscillatory strain sweep and frequency sweep were employed in the measurements (Fig. 2). The rheological parameters, storage modulus (G′) and loss modulus (G″), representing the deformation energy stored and dissipated during the shearing process, respectively, were evaluated [49]. The linear viscoelastic (LVE) regimes of hydrogels were identified through strain sweep tests (Fig. 2A), indicating that G′ and G″ were relatively independent of the applied strain in the range of 0.001 %–10 %. This observation demonstrated the ability of the hydrogels to maintain their gel properties within the tested strain range.

To compare G′ and G″ values, the viscoelastic properties of these assembled hydrogels were systematically explored using dynamic frequency sweep within the LVE regime, which allowed for providing insights into the mechanical stiffness of these hydrogels. Results demonstrated that both G′ and G″ were almost frequency-independent within the tested range of 0.1 Hz–100 Hz, with G′ consistently higher than G″ in all hydrogels, emphasizing their predominantly elastic behaviors (Fig. 2B). A statistical study on G′ values obtained from the frequency sweep indicated the formation of the weakest hydrogel at a peptide ratio of 1:1 than at the other ratios (0:1, 1:3, 3:1 and 1:0) (Fig. 2C). At a specific point, e. g. 0.2 % strain and 1 Hz frequency, there are differences in the modulus values of hydrogels between Fig. 2A and B. It is worth noting that, although the test parameters seemed identical, the moduli were obtained from two scanning modes. Such differences are generally acceptable. Here we only compared the modulus obtained from the frequency sweep mode. These findings suggested that the mechanical properties of the hydrogels were influenced by the mixing ratios of ecf-5 and ECF-5. That is, altering the molar ratios of chiral peptides emerged as a valuable approach to regulating the mechanical strength of supramolecular hydrogels.

As shown in Fig. S1, the gel-sol transition of all hydrogels occurred at around 110 °C, as evidenced by a sharp decrease in both G′ and G″. The recovery properties of the hydrogels were also determined by time-dependent step-strain rheological experiments (Fig. S2). The results showed that the value of G′ was higher than that of G″ in the first stage at a strain of 0.2 %. A large deformation (G′ < G″) occurred when the strain increased to 200 % in the second stage. When the strain suddenly decreased to a constant low level of 0.2 %, hydrogel recovery was evidenced by the higher value of G′ than G″.

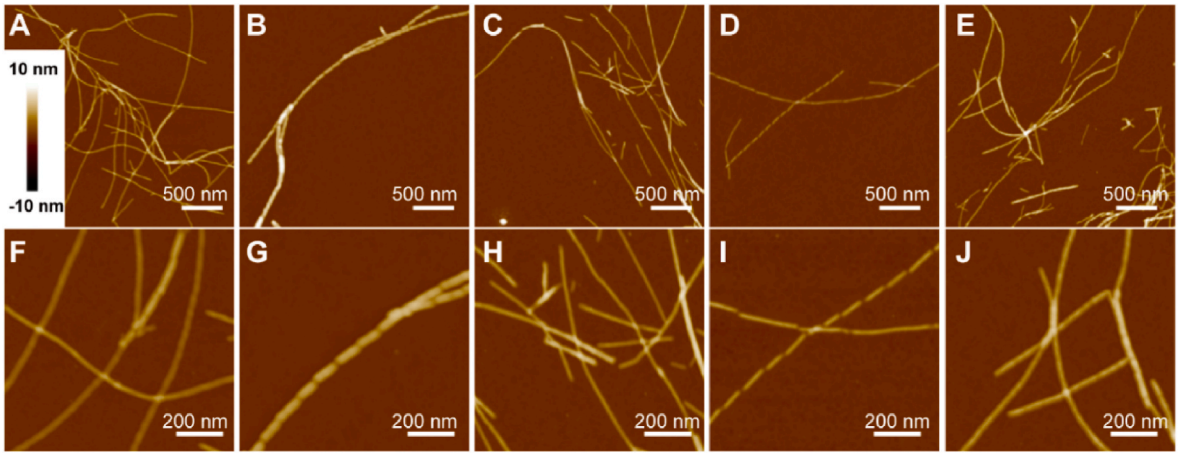

Fig. 4. AFM images of peptide nanostructures formed by ecf-5 and ECF-5 at various ratios. (A) and (F) 0:1, (B) and (G) 1:3, (C) and (H) 1:1, (D) and (I) 3:1, (E) and (J) 1:0.

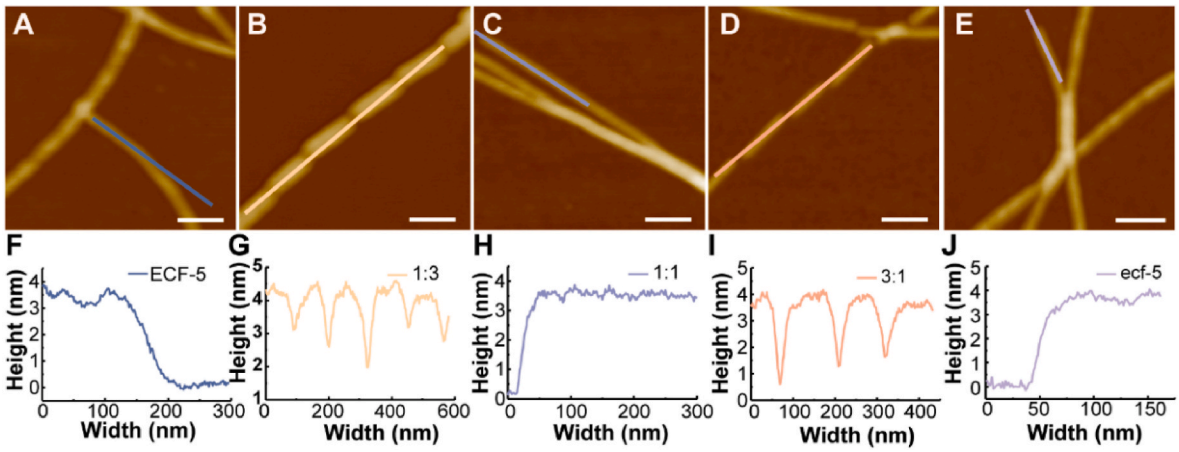

Fig. 5. AFM images and the height profiles of the corresponding fibrils marked at AFM images. (A–E) AFM imaging of fibrils formed by chiral peptides at various mixing ratios. (F–J) Height profiles along the colored lines shown in A-E. The length scale bars are 100 nm.

3.2. Morphologies of peptide assemblies

The successful development of a mechanically self-supporting peptide hydrogel relies on the synergetic effects of peptide-peptide and peptide-solvent interactions, along with the number of cross-links established by fibers in the network and the stiffness of individual fibers [48]. It is imperative to elucidate the entanglement of peptide fibrils and the arrangement of peptide molecules along these fibrils. In pursuing this understanding, a comprehensive investigation of nanostructures formed by ecf-5 and ECF-5 at various ratios was conducted using SEM, negative-stain TEM and AFM.

SEM images showed fiber bundles and pores at all mixing ratios (Fig. 3A-E). TEM studies revealed tightly intertwined fibrils formed by ecf-5 and ECF-5 at ratios of 0:1, 1:3, 3:1 and 1:0 (Fig. 3F, G, 3I, and 3J), while sparse fibrils were observed at a peptide ratio of 1:1 (Fig. 3H). Numerous morphological characterizations of the peptide assemblies were identified using TEM and AFM (featured in Fig. 3 and S3), consistently indicating a smaller degree of fibril entanglement at a 1:1 peptide ratio than that in the other ratios. The formation of fewer intertwined fibrils at a ratio of 1:1 could be one of the reasons for the lower mechanical strength of the peptide hydrogel compared with those formed at the other ratios.

To acquire detailed information of the nanostructures of fibrils, AFM imaging was also carried out. We found that smooth fibrils were formed

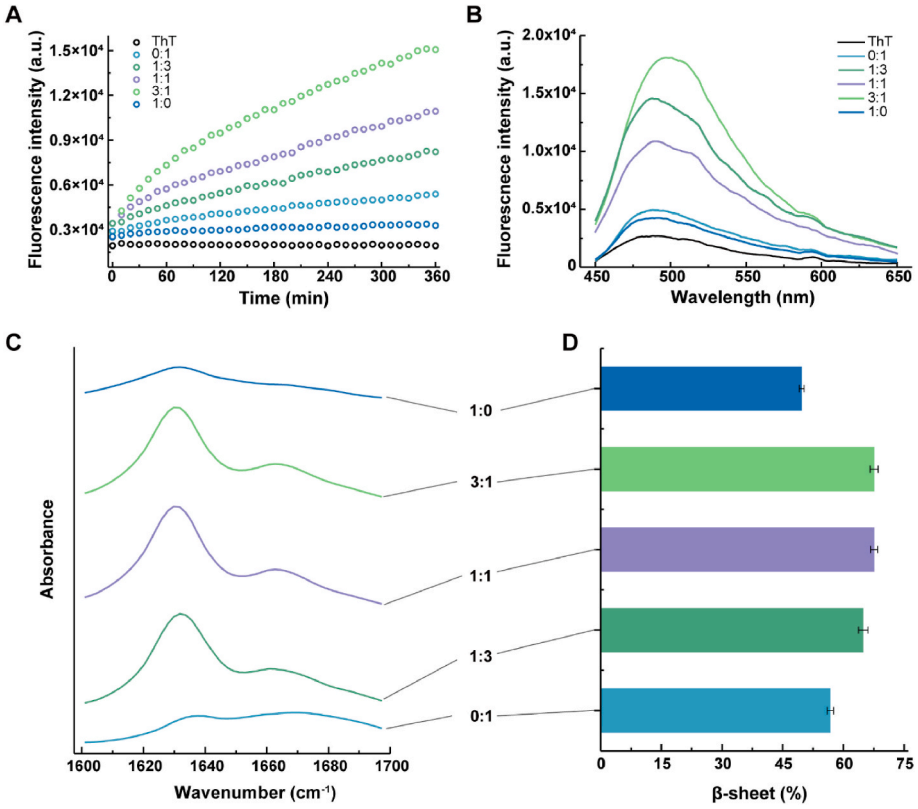

Fig. 6. The formation of β-sheet conformation in the mixture of the enantiomeric peptides ecf-5 and ECF-5 at various ratios. (A) The evolution of ThT fluorescence intensity in the peptide solutions. (B) ThT fluorescence spectra in the peptide solutions. (C) FTIR spectra from the peptide hydrogels. (D) The contents of the β-sheet secondary structures in the in the mixture of the enantiomeric peptides.

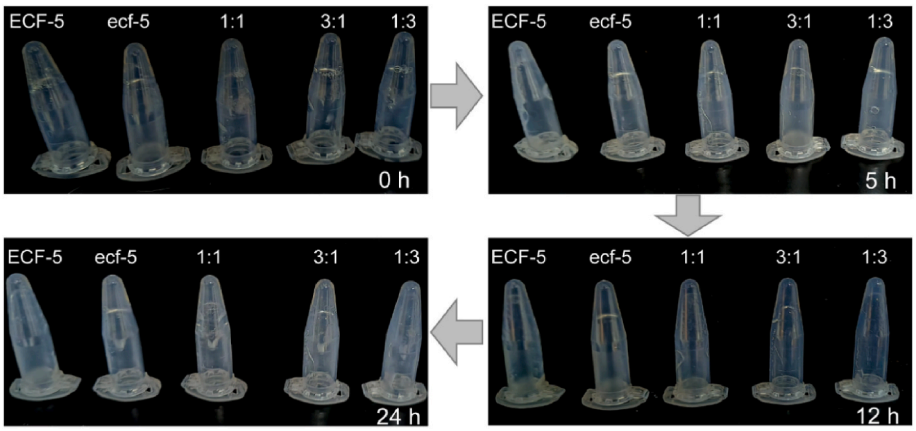

Fig. 7. Photographs of inverted tubes indicating proteolytic stability of hydrogels formed by ecf-5 and ECF-5 at various ratios. The proteinase K treatment time was labeled at each photograph.

by individual ECF-5 (Fig. 4A and F) and ecf-5 (Fig. 4E and J). Similarly, smooth and continuous fibrils were obtained with mixture of ecf-5 and ECF-5 at a ratio of 1:1 (Fig. 4C and H). In contrast, kinks were observed on peptide fibrils formed by ecf-5 and ECF-5 at ratios of 1:3 and 3:1 (Fig. 4B, G, 4D, and 4I). The apparent height of the fibrils formed at various ratios was approximately 4 nm (Fig. 5A-J), with a full width at half maximum (FWHM) of single fibril measuring 30–40 nm. The length of the fragments between the kinks on the peptide fibrils formed at ratios of 1:3 and 3:1 was about 100 nm. The multiplicity of fibril morphology led us to propose the co-assembly of chiral peptides at various ratios to produce two-component fibrils.

3.3. Secondary structures of co-assembling chiral peptides

The enantiomeric peptides, ecf-5 and ECF-5, contain a Phe-Phe motif that inclines them toward adopting a β-sheet conformation and self-assembling into fibers, ultimately forming hydrogels [47]. Therefore, it is necessary to investigate the alterations in secondary structures and the evolution of the assembly process when introducing the enantiomer into its self-assembling system. To this end, ThT fluorescence spectroscopy and FTIR analysis were carried out. Firstly, the formation of β-sheet structures and the assembly kinetics of the enantiomeric peptides ecf-5 and ECF-5 at various ratios were monitored using ThT dye, with an excitation at 440 nm and an emission at 485 nm. ThT fluorescence intensity was recorded over time to determine the assembly kinetics of the peptides (Fig. 6A). Obviously, the nucleation of the chiral peptide was quite fast, quickly reaching a plateau in the kinetic curve. As evidenced by the increasing fluorescence intensity in all samples over time, these peptides were predominant in β-sheet structures. Notably, mixture of chiral peptides exhibited higher ThT fluorescence intensities compared with that of the single-component peptides, emphasizing their superior ability to collaboratively transform into β-sheet structures and co-assemble into fibrils. ThT fluorescence spectra of the peptide mixture at various ratios further supported this observation (Fig. 6B) and showed higher intensities than those of the single-component peptides, implying that mixed chiral peptides tended to form more β-sheet structures than their single-component counterparts.

Subsequently, FTIR spectra of the hydrogels were recorded to identify the secondary structures of chiral peptides at various ratios. The curves of all hydrogels exhibited similar shapes in the wavelength range of 1600–1700 cm^{-1} (Fig. 6C), in which the peak around 1635 cm^{-1} was attributed to the hydrogen-bonded stretching of the amide group closed to the benzene core of the peptides [50,51]. The absorption intensities for the hydrogen-bonded amide C═O, located at around 1635 cm^{-1}, were higher in the peptide mixture at ratios of 3:1,1:3 and 1:1 than at ratios of 1:0 and 0:1, suggesting a greater tendency for co-assembly than self-assembly. FTIR peak deconvolution was applied to analyze the secondary structure distribution (Fig. 6D) [52], revealing that the contents of β-sheet secondary structures were 56.8 ± 0.8 % (ECF-5) and 49.7 ± 0.6 % (ecf-5), respectively. Higher proportions of β-sheet structures were obtained in peptide mixture at ratios of 1:3 (64.9 ± 1.2 %), 1:1 (67.6 ± 0.9 %) and 3:1 (67.6 ± 1.0 %), illustrating a heightened tendency for β-sheet formation by co-assembly (1:3, 1:1 and 3:1) compared with the self-assembly of chiral peptides. These findings were consistent with ThT fluorescence analysis. However, the highest content of β-sheet secondary structures in the peptide mixture at a ratio of 1:1 seemed contradictory to the fact that it formed weakest hydrogel compared with the other ratios (Fig. 2C). Probably, in addition to the content of β-sheet, other factors such as fibril-fibril interactions and fibril-water interactions would also affect hydrogel mechanical properties.

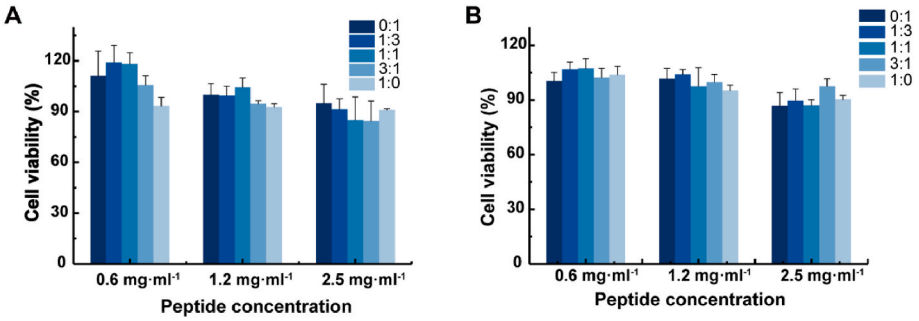

Fig. 8. The cytotoxicity of ecf-5 and ECF-5 mixture at various ratios determined by CCK-8 test. (A) MIN6 cells. (B) HUVECs cells. The total peptide concentrations of 0.6 mg ml^{-1}, 1.2 mg ml^{-1} and 2.5 mg ml^{-1}, respectively, were used in the experiments.

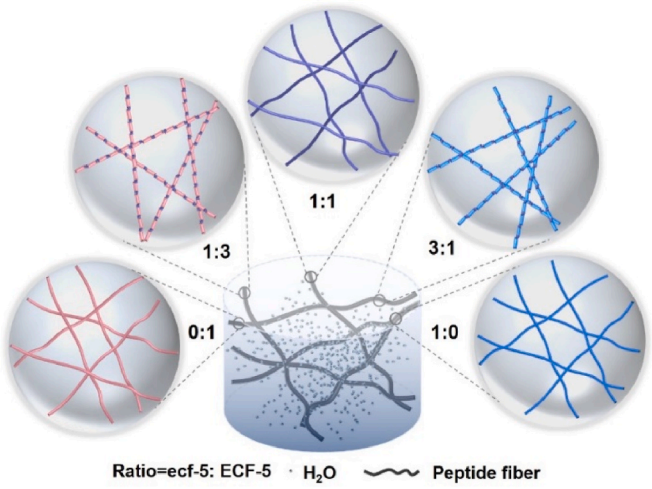

Scheme 1. The proposed mechanism of the fibril formation with ecf-5 and ECF-5 at various ratios.

3.4. Enzymatic digestion of hydrogels and cell compatibility evaluation

The biostability of hydrogels formed by chiral peptides was evaluated by introducing protease K into the hydrogels. The ecf-5 hydrogel displayed a stronger resistance to proteolytic digestion, as reflected in the well-defined solid-like hydrogel morphology after 24 h of treatment. Conversely, the ECF-5 hydrogel collapsed into a solution after 5 h treatment with protease K (Fig. 7). In the case of the hydrogels formed by mixture of ecf-5 and ECF-5, increased resistance to proteolytic digestion was observed with the addition of ecf-5 to ECF-5 peptide. The greater the proportion of ecf-5 peptide in the mixture, the higher the biostability of the hybrid peptide hydrogel. Based on this observation, a potential dose-dependent relationship between peptide concentration and biostability was established, which suggested a pathway for formulating hydrogels with tailored ecf-5 peptide concentrations to achieve optimal biostability in specific biological applications.

To evaluate the cytotoxicity, CCK-8 assay was employed in both MIN6 and HUVEC cells, treated with mixture of ecf-5 and ECF-5 at various ratios. Fig. 8A revealed that more than 80 % of the cells survived after 24 h of co-culture with the peptide mixture, even at a peptide concentration of up to 2.5 mg ml^{-1}. Similar viability was observed in HUVEC cells treated with the peptide mixture (Fig. 8B). These results demonstrated the biocompatibility of the diverse ratios of ecf-5 and ECF-5 mixture, suggesting their great potential for biomedical applications.

4. Discussion

Based on the gelation behaviors, rheological strength of the peptide hydrogels, and the diverse morphologies of peptide assemblies formed by ecf-5 and ECF-5 at various ratios, a compelling inference emerged. The hybrid nature of the chiral peptides significantly influenced the intermolecular packing manner, giving rise to distinct nanostructures [7]. These subtle morphological alterations at the microscopic level may account for the varied macroscopic gelation behaviors of the corresponding hydrogels [53].

To our knowledge, Scheme 1 depicted a proposed mechanism for the hierarchical assembly of chiral peptides. It elucidated the occurrence of co-assembly between the two enantiomers, with the resulting assembled structures being fine-tuned by the mixing ratios [14]. Specifically, uniform and hybrid fibrils were formed by ecf-5 and ECF-5 at a ratio of 1:1[55]. However, when the amounts of ecf-5 and ECF-5 were unequal, the redundancy of one enantiomer prompted its self-assembly, leading to an alternating arrangement of the co-assembled and self-assembled peptide fragments. This was evidenced by the observed kinked fibrils formed by ecf-5 and ECF-5 at ratios of 3:1 and 1:3. The difference in morphologies of fibrils and the formation of kinks led us to propose that the kinked part might arise from the co-assembly of the two peptides, while the self-assembly of the redundant peptides in the enantiomers could be a possible reason for the formation of the fragments between the kinks on the fibrils.

If this is the case, the fragments between the kinks would be longer when the ratio of the two peptides deviated further from 1:1. As depicted in Fig. 9, the fragments on the peptide fibrils between the kinks were approximately 150 nm, obtained at ratios of 1:9 and 9:1, considerably longer than those observed at ratios of 1:3 and 3:1 (~100 nm), providing support for our hypothesis. The lengths of the kinked parts were not compared due to potential effect of AFM tip convolution on accurate measurements of the relatively short parts.

5. Conclusions

In conclusion, we investigated the supramolecular structures and hydrogel properties resulting from the assembly of a pair of enantiomeric peptides, ecf-5 and ECF-5, at various molar ratios. The consistent formation of hybrid β-sheet fibril networks characterized all co-assembled hydrogels. Compared with smooth and continuous fibrils formed at ratios of 1:0, 1:1 and 1:0, distinct fragments of approximately 100 nm in length, separated by kinks, were observed in the peptide mixture at ratios of 1:3 and 3:1. This morphological diversity was attributed to the alternating arrangement of the co-assembled and self-assembled peptide fragments. The significantly lower mechanical properties were achieved in 1:1 hydrogel than those of 3:1 and 1:3. A potential dose-dependent relationship between ecf-5 concentration and resistance to proteolytic digestion was established in these hybrid hydrogels with biocompatibility in both MIN6 and HUVECs cells. These findings present a new perspective on fine-tuning the mechanical properties and supramolecular structures of peptide-based hydrogels, which hold great promise for applications in material and biological sciences.

CRediT authorship contribution statement

Tingyuan Tan: Conceptualization, Data curation, Formal analysis, Investigation, Methodology, Visualization, Writing – original draft.

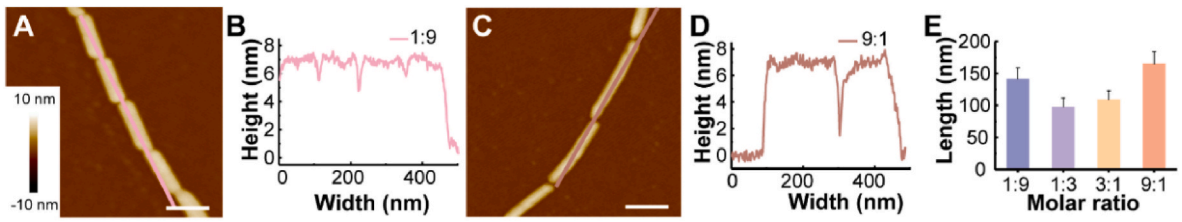

Fig. 9. (A, C) AFM images of peptide fibrils formed with ecf-5 and ECF-5 and (B, D) the corresponding height profiles along the lines shown in (A, C). The ratios of ecf-5 and ECF-5 in the mixture are 1:9 (A–B) and 9:1 (C–D), respectively. (E) The length of fragment between kinks on the peptide fibrils formed with ecf-5 and ECF-5 at unequal ratios. The length scale bars in (A) and (C) are 100 nm.

Yangqian Hou: Data curation, Formal analysis, Writing – review & editing. **Jiali Shi:** Data curation, Investigation. **Biao Wang:** Methodology, Writing – review & editing, Supervision. **Yi Zhang:** Conceptualization, Funding acquisition, Supervision, Writing – review & editing.

Declaration of competing interest

The authors declare that they have no known competing financial interests or personal relationships that could have appeared to influence the work reported in this paper.

Data availability

Data will be made available on request.

Acknowledgements

Financial support received from the National Natural Science Foundation of China (Nos. 11975297) is acknowledged.

Appendix A. Supplementary data

Supplementary data to this article can be found online at https://doi.org/10.1016/j.mtbio.2024.100961.

References

[1] M. Liu, L. Zhang, T. Wang, Supramolecular chirality in self-assembled systems, Chem. Rev. 115 (15) (2015) 7304–7397.
[2] S.M. Morrow, A.J. Bissette, S.P. Fletcher, Transmission of chirality through space and across length scales, Nat. Nanotechnol. 12 (5) (2017) 410–419.
[3] Y. Zheng, Y. Kobayashi, T. Sekine, et al., Visible chiral discrimination via macroscopic selective assembly, Commun. Chem. 1 (1) (2018) 4.
[4] X. Dou, N. Mehwish, C. Zhao, et al., Supramolecular hydrogels with tunable chirality for promising biomedical applications, Acc. Chem. Res. 53 (4) (2020) 852–862.
[5] Y. Zheng, K. Mao, S. Chen, et al., Chirality effects in peptide assembly structures, Front. Bioeng. Biotechnol. 9 (2021) 703004.
[6] R. Mahalakshmi, P. Balaram, The Use of D-Amino Acids in Peptide Design, 2007.
[7] X. Yang, H. Lu, Y. Tao, et al., Controlling supramolecular filament chirality of hydrogel by co-assembly of enantiomeric aromatic peptides, J. Nanobiotechnol. 20 (1) (2022) 77.
[8] R. Appavu, C.B. Chesson, A.Y. Koyfman, et al., Enhancing the magnitude of antibody responses through biomaterial stereochemistry, ACS Biomater. Sci. Eng. 1 (7) (2015) 601–609.
[9] S. Marchesan, Y. Qu, L.J. Waddington, et al., Self-assembly of ciprofloxacin and a tripeptide into an antimicrobial nanostructured hydrogel, Biomaterials 34 (14) (2013) 3678–3687.
[10] Z. Guo, Y. Wang, T. Tan, et al., Antimicrobial d-peptide hydrogels, ACS Biomater. Sci. Eng. 7 (4) (2021) 1703–1712.
[11] Y. Wang, W. Qi, R. Huang, et al., Rational design of chiral nanostructures from self-assembly of a Ferrocene-modified dipeptide, J. Am. Chem. Soc. 137 (24) (2015) 7869–7880.
[12] T. Ishigami, K. Suga, H. Umakoshi, Chiral recognition of L-amino acids on liposomes prepared with L-phospholipid, ACS Appl. Mater. Interfaces 7 (38) (2015) 21065–21072.
[13] J. Jiang, Y. Meng, L. Zhang, et al., Self-assembled single-walled metal-helical nanotube (M-HN): creation of efficient supramolecular catalysts for asymmetric reaction, J. Am. Chem. Soc. 138 (48) (2016) 15629–15635.
[14] M.T. Jeena, K. Jeong, E.M. Go, et al., Heterochiral assembly of amphiphilic peptides inside the mitochondria for supramolecular cancer therapeutics, ACS Nano 13 (10) (2019) 11022–11033.
[15] Y.Y. Xie, X.T. Qin, J. Zhang, et al., Self-assembly of peptide nanofibers with chirality-encoded antimicrobial activity, J. Colloid Interface Sci. 622 (2022) 135–146.
[16] C. Xing, H. Zhu, X. Dou, et al., Infected diabetic wound regeneration using peptide-modified chiral dressing to target revascularization, ACS Nano 17 (7) (2023) 6275–6291.
[17] Z. Guo, Y. Song, Y. Wang, et al., Macrochirality of self-assembled and co-assemled supramolecular structures of a pair of enantiomeric peptides, Front. Mol. Biosci. 8 (2021) 700964.
[18] G.F. Liu, D. Zhang, C.L. Feng, Control of three-dimensional cell adhesion by the chirality of nanofibers in hydrogels, Angew. Chem., Int. Ed. 53 (30) (2014) 7789–7793.
[19] S. Kralj, O. Bellotto, E. Parisi, et al., Heterochirality and halogenation control Phe-Phe hierarchical assembly, ACS Nano 14 (12) (2020) 16951–16961.
[20] O. Chaudhuri, J. Cooper White, P.A. Janmey, et al., Effects of extracellular matrix viscoelasticity on cellular behaviour, Nature 584 (7822) (2020) 535–546.
[21] C. Ligorio, A. Mata, Synthetic extracellular matrices with function-encoding peptides, Nat. Rev. Bioeng. 1 (2023) 518–536.
[22] A. Levin, T.A. Hakala, L. Schnaider, et al., Biomimetic peptide self-assembly for functional materials, Nat. Rev. Chem 4 (11) (2020) 615–634.
[23] E. Prince, E. Kumacheva, Design and applications of man-made biomimetic fibrillar hydrogels, Nat. Rev. Mater. 4 (2) (2019) 99–115.
[24] F. Gelain, Z. Luo, S. Zhang, Self-assembling peptide EAK16 and RADA16 nanofiber scaffold hydrogel, Chem. Rev. 120 (24) (2020) 13434–13460.
[25] R. Chang, X. Yan, Supramolecular immunotherapy of cancer based on the self-assembling peptide design, Small Struct. 1 (2) (2020) 2000068.
[26] X. Du, J. Zhou, J. Shi, et al., Supramolecular hydrogelators and hydrogels: from soft matter to molecular biomaterials, Chem. Rev. 115 (24) (2015) 13165–13307.
[27] S. Talebian, M. Mehrali, N. Taebnia, et al., Self-healing hydrogels: the next paradigm shift in tissue engineering? Adv. Sci. 6 (16) (2019) 1801664.
[28] D.R. Griffin, M.M. Archang, C.H. Kuan, et al., Activating an adaptive immune response from a hydrogel scaffold imparts regenerative wound healing, Nat. Mater. 20 (4) (2021) 560–569.
[29] P. Makam, E. Gazit, Minimalistic peptide supramolecular co-assembly: expanding the conformational space for nanotechnology, Chem. Soc. Rev. 47 (10) (2018) 3406–3420.
[30] R.J. Swanekamp, J.T.M. DiMaio, C.J. Bowerman, et al., Coassembly of enantiomeric amphipathic peptides into Amyloid-inspired rippled β-sheet fibrils, J. Am. Chem. Soc. 134 (12) (2012) 5556–5559.
[31] Q. Wang, Y. Zhang, Y. Ma, et al., Nano-crosslinked dynamic hydrogels for biomedical applications, Mater. Today Bio (2023) 100640.
[32] A. Lakshmanan, D.W. Cheong, A. Accardo, et al., Aliphatic peptides show similar self-assembly to amyloid core sequences, challenging the importance of aromatic interactions in amyloidosis, Proc. Natl. Acad. Sci. U. S. A. 110 (2) (2013) 519–524.
[33] P.W. Frederix, G.G. Scott, Y.M. Abul Haija, et al., Exploring the sequence space for (tri-)peptide self-assembly to design and discover new hydrogels, Nat. Chem. 7 (1) (2015) 30–37.
[34] D.E. Clarke, C.D.J. Parmenter, O.A. Scherman, Tunable pentapeptide self-assembled β-sheet hydrogels, Angew. Chem., Int. Ed. 57 (26) (2018) 7709–7713.
[35] W.T. Truong, Y. Su, D. Gloria, et al., Dissolution and degradation of Fmoc-diphenylalanine self-assembled gels results in necrosis at high concentrations in vitro, Biomater. Sci. 3 (2) (2015) 298–307.
[36] A.D. Martin, P. Thordarson, Beyond Fmoc: a review of aromatic peptide capping groups, J. Mater. Chem. B 8 (5) (2020) 863–877.
[37] J.P. Wojciechowski, A.D. Martin, A.F. Mason, et al., Choice of capping group in tripeptide hydrogels influences viability in the three-dimensional cell culture of tumor spheroids, ChemPlusChem 82 (3) (2017) 383–389.
[38] Y. Yuan, Y. Shi, J. Banerjee, et al., Structuring supramolecular hyaluronan hydrogels via peptide self-assembly for modulating the cell microenvironment, Mater. Today Bio (2023) 100598.
[39] N. Yadav, M.K. Chauhan, V.S. Chauhan, Short to ultrashort peptide-based hydrogels as a platform for biomedical applications, Biomater. Sci. 8 (1) (2020) 84–100.
[40] M. Melchionna, K.E. Styan, S. Marchesan, The unexpected advantages of using D-amino acids for peptide self- assembly into nanostructured hydrogels for medicine, Curr. Top. Med. Chem. 16 (18) (2016) 2009–2018.
[41] A. García Fernández, D. Iglesias, E. Parisi, et al., Chirality effects on peptide self-assembly unraveled from molecules to materials, Chem 4 (2018) 1862–1876.
[42] T.M. Clover, C.L. O'Neill, R. Appavu, et al., Self-assembly of block heterochiral peptides into helical tapes, J. Am. Chem. Soc. 142 (47) (2020) 19809–19813.
[43] J. Lu, H. Xu, J. Xia, et al., D- and unnatural amino acid substituted antimicrobial peptides with improved proteolytic resistance and their proteolytic degradation characteristics, Front. Microbiol. 11 (2020) 563030.
[44] P. Xing, Y. Zhao, Controlling supramolecular chirality in multicomponent self-assembled systems, Acc. Chem. Res. 51 (9) (2018) 2324–2334.
[45] K.J. Nagy, M.C. Giano, A. Jin, et al., Enhanced mechanical rigidity of hydrogels formed from enantiomeric peptide assemblies, J. Am. Chem. Soc. 133 (38) (2011) 14975–14977.
[46] Z. Shen, Z. Guo, T. Tan, et al., Reactive oxygen species scavenging and biodegradable peptide hydrogel as 3D culture scaffold for Cardiomyocytes, ACS Biomater. Sci. Eng. 6 (7) (2020) 3957–3966.
[47] I. Coin, M. Beyermann, M. Bienert, Solid-phase peptide synthesis: from standard procedures to the synthesis of difficult sequences, Nat. Protoc. 2 (12) (2007) 3247–3256.
[48] D.E. Clarke, E.T. Pashuck, S. Bertazzo, et al., Self-healing, self-assembled β-sheet peptide-poly (γ-glutamic acid) hybrid hydrogels, J. Am. Chem. Soc. 139 (21) (2017) 7250–7255.
[49] M. Zhou, A.M. Smith, A.K. Das, et al., Self-assembled peptide-based hydrogels as scaffolds for anchorage-dependent cells, Biomaterials 30 (13) (2009) 2523–2530.
[50] X. Liu, J. Fei, A. Wang, et al., Transformation of dipeptide-based organogels into chiral crystals by cryogenic treatment, Angew. Chem., Int. Ed. 56 (10) (2017) 2660–2663.
[51] A. Baral, S. Basak, K. Basu, et al., Time-dependent gel to gel transformation of a peptide based supramolecular gelator, Soft Matter 11 (24) (2015) 4944–4951.
[52] K. Elfrink, J. Ollesch, J. Stöhr, et al., Structural changes of membrane-anchored native PrPC, Proc. Natl. Acad. Sci. U. S. A. 105 (31) (2008) 10815–10819.
[53] G. Zhang, L. Zhang, H. Rao, et al., Role of molecular chirality and solvents in directing the self-assembly of peptide into an ultra-pH-sensitive hydrogel, J. Colloid Interface Sci. 577 (2020) 388–396.